Methamphetamine drug abuse and addiction: Effects on face asymmetry

Mohamad Harastani, Amine Benterkia, Farnaz Majid Zadeh, Amine Nait-Ali

Version of Record: https://www.sciencedirect.com/science/article/pii/S0010482519303452
Manuscript_d76cf1f950834d7e9a0814de2d7eda6a

Methamphetamine Drug Abuse and Addiction: Effects on Face Asymmetry

Mohamad Harastani, Amine Benterkia, Farnaz Majid Zadeh, Amine Nait-Ali*

Université Paris-Est Créteil, Faculty of Sciences and Technology, International Master of Biometrics, 61 Avenue du Général de Gaulle, 94010 Créteil Cedex, France

Abstract

The abnormal aging mechanism associated with drug abuse results in poor performance of face recognition systems on illicit drug addicts (mainly methamphetamine). Consequently, the high correlation between drug addiction and crime exaggerates the urge for further investigations to originate and overcome this problem. Concurrently, face asymmetry was found to play a significant role in face recognition and age estimation. Therefore, facial asymmetry assessment for meth-addicts is highly serviceable, acknowledging how meth addiction accelerates biological aging and causes severe face distortion. In this work, we address facial asymmetry for meth-addicts compared with ordinary people.

We assess facial asymmetry by employing the most credible state-of-the-art tools for local and global two-dimensional (2D) methods. More specifically, we use a classical bilateral-based metric for local analysis, combined with a proposed global approach, that we refer to as the Area Mismatch metric, to give a vivid overview of geometrical facial asymmetry. Finally, we construct a metric for textural facial asymmetry assessment by employing the Structural Similarity Index (SSIM) for dual regions in a given face.

We apply the aforementioned metrics on two databases, a recently collected meth-addicted database and a regular aging database (FERET). Statistical analysis indicated a significant increment of facial asymmetry for meth addicts

*Corresponding author
Email address: naitali@u-pec.fr (Amine Nait-Ali)

while aging, three to five times more than ordinary people.

This study definitively answers the question regarding the correlation between meth abuse and addiction and the increase of facial asymmetry. Also, it confirms previous findings concerning aging and increased facial asymmetry.

Keywords: Facial Asymmetry, Drug Addiction, Methamphetamine, Aging, Biometrics

1. Introduction

Face perception is a complex process that the human brain does effortlessly abreast of machines. In fact, humans are capable of recognizing faces against temporal variations to a certain extent, that machines are not yet able to catch up, even for faces that *"aged well"* [1]. Moreover, the challenge of face recognition against temporal variations exaggerates for faces that *"aged badly"*. Whilst illicit drug abuse and addiction have serious impacts on the characteristics of faces [2, 3] (Figure 1(b)). As a result, face recognition systems have witnessed poor performance for drug addicts [4, 5, 6, 7]. Consequently, the high correlation between drug addiction and crime augments the need for further investigations to cope with this problem.

Laterally in [8], it has been shown that face asymmetry increases with aging. Where the lower hemifaces were concluded to exhibit maximum asymmetry across temporal variations. When taking into account that drug addiction accelerates biological aging [9], combining it with the effects of methamphetamine (meth) on the faces of its addicts (in 1.1) and finally, considering that there is a high correlation between face symmetry and recognition, it seems to be very critical to quantify the aforementioned asymmetry for meth-addicts.

1.1. Meth effects on faces

From a survey on medical and health-related articles [2, 3] meth abuse relates to the following effects on faces:

- Mouth: severe teeth decay, known as the *meth-mouth* effect. This is due to the corrosive nature of the drug, which unbalances the lips and mandibular symmetry while increasing the chances for infections and face swells.
- Eyes: dark circles under the eyes.
- Nose: severe runny nose causing nose-bleed, which results in nose irritations and swells.
- Skin health: sores and intensive itching, which leaves face marks in the form of severe acne and wounds.
- Wrinkles: loss of soft tissues and body fat accompanied by a severe weight loss, due to the loss of appetite associated with meth use.

It is worth mentioning that face symmetry distortion is usually witnessed with patients that went through some serious medical treatments, such as radiotherapy, chemotherapy and surgery [10].

In this work, face asymmetry for illicit drug addicts (mainly meth) is assessed by employing the most credible state-the-of-art tools for local and global 2D face symmetry assessment. More specifically, the use of a classical bilateral-based metric for local analysis is combined with a proposed global approach that we name as the Area Mismatch metric to give a vivid overview of face geometrical symmetry. Moreover, a metric for textural face symmetry is constructed by employing the Structural Similarity Index (SSIM) for dual regions in a given face. Lastly, the aforementioned metrics are applied to two databases, a recently collected illicit drug-addicted database and an ordinary aging database (FERET). The statistical results were analyzed to answer the question *does meth affect face symmetry?*

1.2. related work

According to the recent literature on face asymmetry [11, 12, 13], 3D-based assessment methods have gained popularity in the past decade. Yet, these methods are still confined to clinics and require advanced cameras or CT scans [10, 14]. The aforementioned methods are usually used as assessment tools to threshold the necessity of surgical intervention to restore facial symmetry.

While in the context of addressing the question "*does drug abuse distort face symmetry?*" such 3D models that are captured under highly controlled settings are not yet available. In fact, most of the publicly-available data concerning the aging of drug addicts were collected from mug-shots in the *faces of meth* project [15]. Fortunately, absolute accuracy is not required to answer the previous question. In fact, state-of-the-art 2D face symmetry analysis tools can be effectively employed to answer this question. Some of the methodology developed in this work is inspired by the work done in [8], where the increase of face asymmetry against aging was analyzed using publicly available databases [1]. The key point in this research is to provide a good statistical analysis using widely accepted assessment tools for the data on hand.

It is well known that face symmetry relates to beauty [13]. Hence, most of the developed tools to quantify face symmetry were proposed to threshold the necessity for surgical intervention on several medical cases such as unbalanced mandibular [14], cancer patients after therapy [10] and cleft-lip [11, 16, 17]. While from a technical point of view, face symmetry has been used as a critical factor for several applications. In [18], face symmetry was used to pose correction in 3D face models and improving face recognition. In [19], an optical-flow-based facial symmetry is introduced for face recognition and reconstruction using certain dominant bilateral features that are least affected by pose variations. Others have used face symmetry to improve 3D reconstructed models [20]. However, we find that the most credible 2D face symmetry assessment tool in the medical field is associated with a software known as SymNose [17] which requires manual annotation for the regions of interest (ROIs), and performs an area mismatch measure on the annotated dual face regions. Up to this date, SymNose is still accepted as the most reliable tool to measure 2D face symmetry [16] in the medical field. In contrast with technical papers, where bilateral features are the most used.

To the extent of our knowledge, the only work that performed statistical analysis for face asymmetry across temporal variation from 2D images is done by M. Sajid et al. [8]. In the latter work, geometrical face asymmetry analysis

is used to show aging effects on face symmetry. In our work, we extend their results to include textural asymmetry analysis; then we use our findings to compare with the aging of drug addicts across similar temporal variations.

1.3. Employed databases

Assessing the asymmetry of faces across temporal variations from 2D images requires clear frontal face shots for each individual under consideration, captured in separated time slots. This arises a major difficulty in this research due to the very limited publicly available databases offering such a setting. Nowadays, several aging databases that were collected to model aging are surveyed in [1]. However, only the FERET database in its dup I and dup II directories offers clear frontal images that match with this setting for ordinary people aging. Fortunately, the database that was collected for the illicit drug abusers (mostly meth) is specially designed to model the distortion of faces versus temporal variations and meets the requirement for this research.

In the following subsections, the two used databases are briefed for the reader.

(a) (b)

Figure 1: Sample images of the two employed databases: (a) members of the FERET database in the first row with the same members at different time instances in the second row, (b) members of the Illicit Drug Addicts database in an early stage of drug abuse in the first row and at a later stage in the second row

1.3.1. The Illicit Drug Addicts database

We collected a database from internet photo collections on drug abuse, mainly using the faces of meth project in [15]. Very similar databases were collected and used in previous works [4, 5, 6]; however, none of these databases was made publicly available up to this date.

The collected database has 120 members with two color frontal face shots at least for each member with an average resolution of (572 x 838), which shows the progress of drug abuse and its effect on the addict's face as shown in Figure 1(b).

The collected database has a variety of members which guarantees generality for a range of adults, covering both genders with close percentages. Besides, since its greatest part was collected in the USA, it combines multiple races due to the country's demography.

1.3.2. The FERET database

FERET is a large publicly available database that combines 3540 2D color face images of resolution (512 x 768) for 1196 subjects in the age of 10-70 years. Although it has multiple pose and expression variations, only frontal images were employed in this work. It has two subdirectories titled with dup I and dup II representing temporal variations and are usually used to study the effect of aging on faces. Where dup II is a subset of dup I and contains larger temporal variations. However, 80 subjects are present in dup I with clear frontal face images that were collected at different time instants with a similar range to the data collected for drug addicts. Besides, FERET contains a similar gender percentage. And since it was collected in the USA (similarly to the Illicit Drug Addicts database), we assume that the variety of races is already covered. Moreover, if we consider the similarity of temporal variations in the images for members of the aforementioned databases, we can justify the assumption that usage of this database for the purpose of comparison is valid. A sample of this database is demonstrated in Figure 1(a).

2. Facial asymmetry measurement

In this section, we present facial asymmetry measurement and evaluation for both the drug addicts and ordinary people across temporal variations (aging) on the databases in 1.3, with necessary landmark detection and face pre-processing in the following sub-sections.

2.1. Data preparation

Before applying facial asymmetry metrics on data, pre-processing the input images is necessary to prepare the suitable inputs for the different metrics. This part of the work was mainly done using the Dlib's face landmarks [21] and demonstrated in Figure 2.

We can summarize the pre-processing as following:

1. Face detection and landmarks extraction.
2. Face normalization (align and resize).
3. Face cropping.
4. Extraction of regions of interest (ROIs).

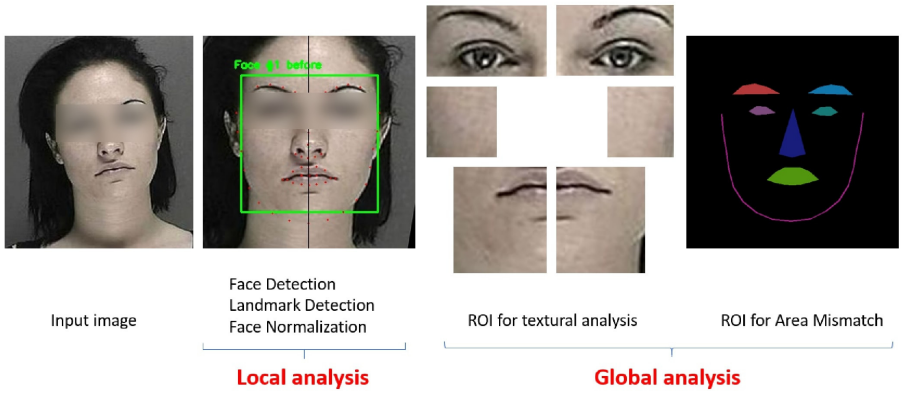

Figure 2: Data pre-processing procedure that runs on all input images

2.1.1. Landmark detection

In this work, we employ the 68-landmarks-extractor of Dlib's implementation in [21] with a shape detector trained on the iBUG 300-W face landmark database [22].

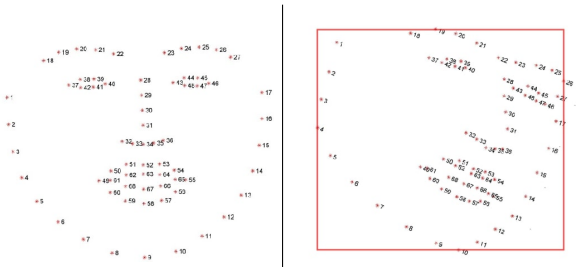

(a) (b)

Figure 3: The 68 face landmarks of Dlib: (a) the landmarks extracted from a frontal face perspective, (b) an illustrative example of face detection and landmark extraction

2.1.2. Face Normalization

For increasing the accuracy of the employed metrics, and due to the nature of the measurements (vertical and horizontal symmetry), the faces must be of the same size and carefully aligned to provide comparable results as shown in Figure 4.

Therefore, affine transformations are used for rotating, scaling and translating in aligning each face using the centers of eyes. This is achieved through finding the rotation angle that makes eye centers lay in the same Y coordinates, then applying a scaling factor to make all output faces in the desired size (300x300). Consequently, an affine transformation matrix M is employed (**rotation** according to the midpoint between eyes centers and **scaling**).

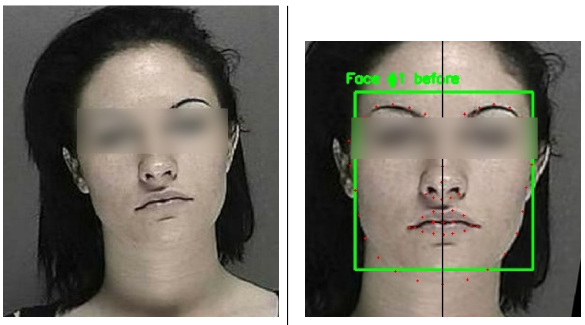

(a) (b)

Figure 4: An illustrative example of affine transformation: (a) an input face image, (b) the same image after affine transformation

2.1.3. Face cropping

In the textural asymmetry measurement (explained later in section 2.3), the right/left dual parts of a given face are compared. Hence, different sub face images are cropped from the normalized face using the coordinates of its landmarks indicated in Table 1 and a demonstration of face cropping in Figure 5.

ROI / Side	Left hemiface	Right hemiface
Eyes	$(X_{18}, Y_{20}) - (X_{18}, Y_{20})$	$(X_{29}, Y_{25}) - (X_{27}, Y_{29})$
Cheeks	$(X_4, Y_{30}) - (X_{49}, Y_4)$	$(X_{55}, Y_{30}) - (X_{55}, Y_{30})$
Mouth	$(X_6, Y_{52}) - (X_9, Y_9)$	$(X_{52}, Y_{52}) - (X_{12}, Y_9)$

Table 1: Landmark coordinates used for cropping dual face regions

(a) (b) (c)

Figure 5: The process of face dual regions extraction: (a) employed landmarks for cropping ROIs, (b) an input image with its corresponding dual regions, (c) dual regions prepared for textural asymmetry analysis

2.1.4. Face region extraction

For the area mismatch metric (explained later in section 2.2.1), regions of the face parts in binary images are needed as input. In contrast with the work done in Symnose [17] where the region of interest are manually annotated, this is automatically achieved using the face landmarks, where the ROIs (eyes, nose, chin, and mouth) were isolated by connecting the landmarks through lines, and the outer perimeter is used as the upper boundary for each region as demonstrated in Figure 6.

(a) (b) (c)

Figure 6: Regions of interest extraction from a given face: (a) an input image, (b) constructing regions of interests, (c) isolating each region of interest for further processing

2.2. Measurement and evaluation of facial asymmetry

In this subsection, the different metrics that are used to measure and quantify face asymmetry are presented. By looking at the databases used in this work, it's easy to notice that the face asymmetry can be affected in both geometrical and textural aspects. Hence, it was necessary to tailor metrics for a relevant evaluation.

- Geometrical asymmetry assessment.

  Bilateral features (local approach).

  Area mismatch (global approach).

- Textural asymmetry assessment.

2.2.1. Geometrical asymmetry assessment

For 2D images, geometrical facial asymmetry measures can be categorized into two main categories, global and local measures.

Local analysis: Bilateral features. The symmetry between the left and right hemifaces is discussed for certain landmarks, for instance, the dual left-right corners of the mouth is a landmark. This type of symmetry measures, usually named as bilateral symmetry. The features are computed using equation 1; each bilateral feature is the percentage of the difference between two bilateral distances (as shown in the Figure7).

$$BF_i\% = \frac{\mid \alpha_i - \beta_i \mid}{\max(\alpha_i, \beta_i)} \times 100 \tag{1}$$

where:

- BF_i : Bilateral feature i.
- α_i : *Midline* to *left feature point* distance for feature i.
- β_i : *Midline* to *right feature point* distance for feature i.

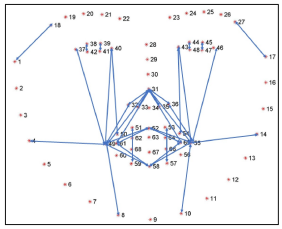

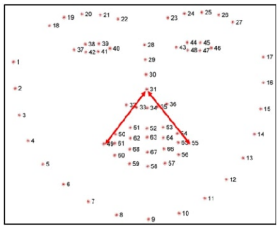

Bilateral Feature	Left Distance	Right Distance
F1	52 – 49	52 – 55
F2	52 – 61	52 – 65
F3	58 – 49	58 – 55
F4	58 – 61	58 – 65
F5	31 – 36	31 – 32
F6	31 – 33	31 – 35
F7	31 – 49	31 – 55
F8	31 – 61	31 – 65
F9	44 – 48	39 – 41
F10	45 – 47	38 – 42
F11	40 – 49	43 – 55
F12	40 – 50	43 – 54
F13	51 – 59	53 – 57
F14	55 – 10	49 – 8
F15	36 – 55	32 – 49
F16	64 – 67	62 – 67
F17	51 – 68	53 – 66
F18	49 – 60	55 – 56
F19	1 – 18	17 – 27
F20	4 – 49	14 – 55

(a) (b) (c)

Figure 7: Employed bilateral features for face asymmetry analysis: (a) a map of all the distances constituting the bilateral features used for asymmetry analysis, (b) an example of one bilateral features indicated as F7 representing the percentage difference of the distances between the tip of the nose and the corners of the mouth, (c) full description of the employed bilateral features based on the coordinates of Dlib 68-landmarks

Dlib's face landmarks were found to have a precision of 3 to 5 pixels as shown in Figure 8. Hence, in order to make the measurement more accurate, a threshold of 3 pixels was used in measuring distances, in such a way that, a distance of less than (Threshold = 3 pixels) is ignored.

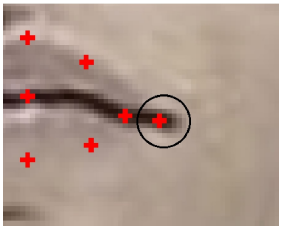

Figure 8: An example on how the precision of a landmark can be in 3 to 5 pixels

An example of the bilateral asymmetry metric applied on two images of the same person in the early and late stages of drug abuse (before and after) is demonstrated in Figure 9.

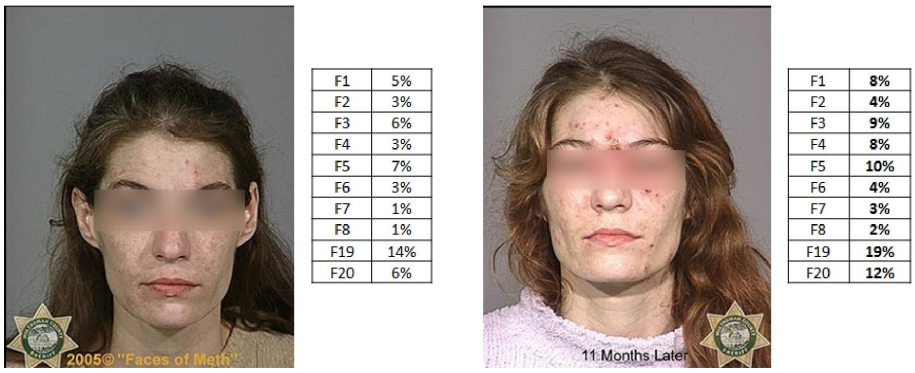

F1	5%
F2	3%
F3	6%
F4	3%
F5	7%
F6	3%
F7	1%
F8	1%
F19	14%
F20	6%

F1	**8%**
F2	**4%**
F3	**9%**
F4	**8%**
F5	**10%**
F6	**4%**
F7	**3%**
F8	**2%**
F19	**19%**
F20	**12%**

Figure 9: Example of bilateral asymmetry features applied on a person in the early and late stages of drug abuse (using equation 1)

Global Analysis: Area mismatch. From a survey on medical research articles, a software named as SymNose is widely accepted to measure the asymmetry in faces from 2D images. SymNose uses the area mismatch concept to give a score on the asymmetry of the nose and upper lip of the two hemifaces of a given face image after performing the ROIs segmentation manually by a user. In this work, the ROIs segmentation is done automatically (as explained in section 2.1.4). The global geometrical asymmetry index is computed following the next steps:

1. Take as an input two regions from the left/right hemifaces.
2. Flip the right ROI.
3. Superimpose the two ROIs (that are supposed to be identical in a symmetric face).
4. Calculate the percentage of mismatched areas using 2.

(a) (b) (c)

Figure 10: Illustration of the area mismatch face asymmetry metric workflow: (a) input ROI, (b) right half flipped, (c) superimposed right/left halfs for comparison

$$AM_{ROI_i}\% = \frac{\lambda_{m_i}}{\lambda_{t_i}} \times 100 \tag{2}$$

where:

- AM_{ROI_i} : Area Mismatch Feature for i^{th} Region of Interest (ROI), where $i \in$ {Mouth, Eyes, Chin, Nose}
- λ_{m_i} : Mismatched Area in the ROI_i
- λ_{t_i} : Total Area of ROI_i

An example of the area mismatch metric applied on two images of the same person in the early and late stages of drug abuse can be found in Figure 11.

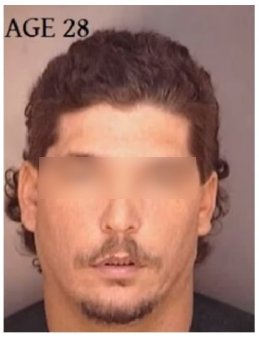

Region	Area mismatch percentage
Mouth	6%
Nose	5%
Eyes	11%
Chin	1%

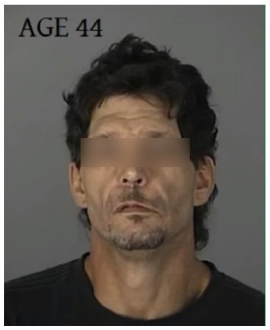

Region	Area mismatch percentage
Mouth	**10%**
Nose	**9%**
Eyes	**14%**
Chin	**5%**

Figure 11: Example of Area Mismatch features applied on a person in the early and late stages of drug abuse

2.3. Textural asymmetry assessment

The textural asymmetry metric is constructed to follow the change in the textural symmetry of a face across temporal variations. The work has been done by employing the structural similarity (SSIM) index formulated in 3. The function takes as an input two images (x,y) of the same size (y is resized to the size of x) and returns the score of similarity of the two input images. The input images here are dual regions from the face as demonstrated in Figure 5(c)

$$SSIM(x, y) := \frac{(2\mu_x\mu_y + c_1)(2\sigma_{xy} + c_2)}{(\mu_x^2 + \mu_y^2 + c_1)(\sigma_x^2 + \sigma_y^2 + c_2)} \tag{3}$$

where:

- μ_x is the average of pixel values in image x.
- μ_y is the average of pixel values in image y.
- σ_x^2 is the pixel variance in image x.
- σ_y^2 is the pixel variance in image y.
- σ_{xy} is the covariance in images x,y.

An example of the textural asymmetry metric applied on two images of the same person in the early and late stages of drug abuse can be found in Figure 12.

Figure 12: Example of textural asymmetry metric applied on a person in the early and late stages of drug abuse

3. Results

The face asymmetry metrics explained in 2.2 were applied on the Dup I directory in the FERET and Illicit Drug Addicts databases explained in 1.3. In the following subsections, the statistical analysis of the results given by these metrics is presented.

3.1. Statistical analysis on the FERET database

To simulate random temporal variations (similar to those exist in the illicit drug addicts database), the results presented in Table 2 were generated with a random selection of before and after shots for the 80 subjects in the Dup I directory of FERET. The results show an increase in facial asymmetry with aging for all metrics.

Moreover, textural analysis demonstrates a textural-wise increase in face asymmetry with normal aging. Precisely, a maximum increase in textural asymmetry was found around the cheeks area. A visual illustration of the findings can be found in the bar graph presented in Figure 13(a). Finally, the cloud representation of the samples is found in Figure 13(b), where it presents the mean values of geometrical versus textural asymmetry, and it shows a slight positive shift on both axes, corresponding to a slight geometrical/textural increment face asymmetry against normal aging.

Feature	Region	Mean Before	SD Before	Mean After	SD After	Before	After	Asymmetry Index
Area Mismatch	Mouth	11%	5%	11%	6%	7%	8%	Geometrical Asymmetry Index
	Nose	15%	8%	16%	9%			
	Eyes	6%	6%	7%	6%			
	Chin	4%	2%	4%	2%			
Bilateral Asymmetry	F1	6%	4%	6%	5%			
	F2	6%	5%	7%	5%			
	F3	5%	4%	6%	4%			
	F4	6%	4%	6%	5%			
	F5	8%	6%	8%	7%			
	F6	4%	4%	6%	5%			
	F7	4%	4%	5%	5%			
	F8	4%	4%	5%	4%			
	F19	11%	8%	14%	9%			
	F20	9%	6%	10%	7%			
Textural Asymmetry	Cheeks	21%	7%	28%	10%	26%	29%	Textural Asymmetry Index
	Eyes	31%	11%	32%	8%			
	Mouth	26%	10%	27%	10%			

Table 2: Statistical results on FERET database

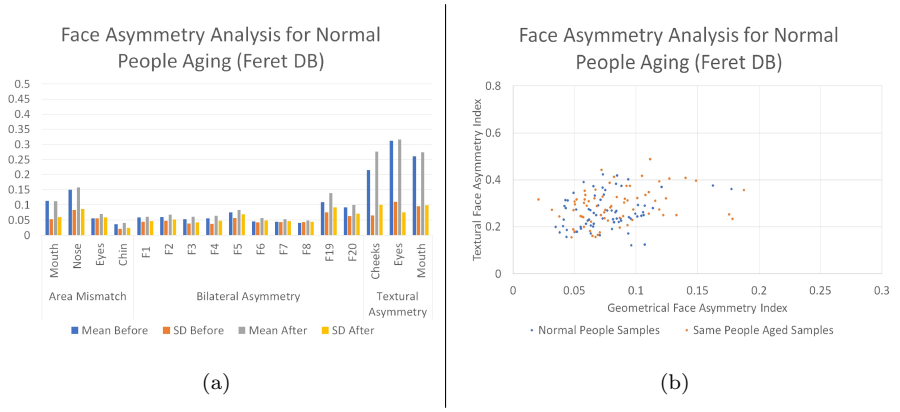

(a) (b)

Figure 13: Demonstrative charts for the statistical results on facial asymmetry analysis on the DUP I FERET database: (a) bar graph representing the statistical results from geometrical and textural analysis, (b) a cloud representation of the samples for geometrical vs textural facial asymmetry

3.2. Statistical analysis on the Illicit Drug Addicts database

The results presented in Table 3 correspond to the before and after images (early vs late stages of drug abuse) of 120 subjects in the Illicit Drug

Addicts database. The results show a significant increase in face asymmetry both geometrical and textural wise with aging, in comparison with the increase of asymmetry in people with normal aging in 3.1. A visual illustration of the findings can be found in the bar graph presented in Figure 14(a). Finally, the cloud representation of the samples used to generate the results in Figure 14(b) presented in geometrical vs textural asymmetry shows a relatively considerable positive shift on both axes when compared with the results obtained on the FERET, indicating the increment of these asymmetry measures.

Feature	Region	Mean Before	SD Before	Mean After	SD After	Before	After	Asymmetry Index
Area Mismatch	Mouth	12%	5%	15%	7%	8%	13%	Geometrical Asymmetry Index
	Nose	16%	9%	20%	11%			
	Eyes	8%	4%	10%	6%			
	Chin	5%	2%	6%	3%			
Bilateral Asymmetry	F1	7%	4%	11%	8%			
	F2	8%	5%	11%	8%			
	F3	6%	5%	9%	7%			
	F4	7%	5%	10%	7%			
	F5	8%	5%	13%	8%			
	F6	5%	4%	8%	5%			
	F7	5%	3%	7%	5%			
	F8	4%	3%	7%	4%			
	F19	14%	11%	21%	14%			
	F20	9%	6%	15%	10%			
Textural Asymmetry	Cheeks	22%	10%	33%	15%	28%	39%	Textural Asymmetry Index
	Eyes	34%	11%	43%	12%			
	Mouth	28%	10%	40%	13%			

Table 3: Statistical results on the Illicit Drug Addicts database

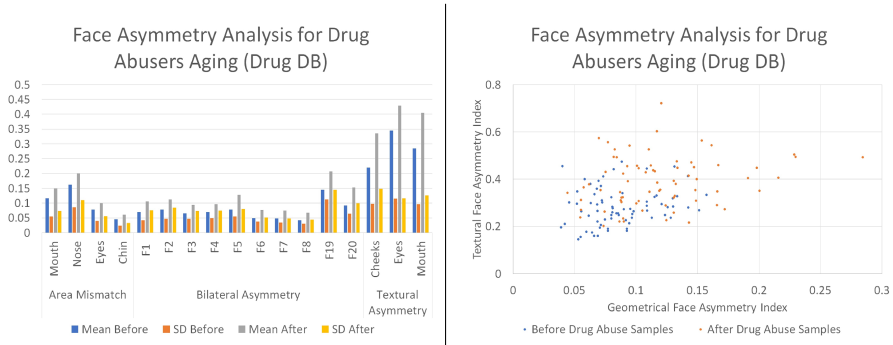

(a) (b)

Figure 14: Demonstrative charts for the statistical results on facial asymmetry analysis on the Drug Addicts database: (a) bar graph representing the statistical results from geometrical and textural analysis, (b) a cloud representation of the samples for geometrical vs textural facial asymmetry

3.3. Statistical comparison: Normal vs Drug-life aging

The results presented in the previous two subsections show that face asymmetry has increased in both normal and drug-life aging. However, in this section, the results are aligned with each other to give a relative comparison and visualization. In Table 4, the standard deviation that was used to validate the findings is dropped from the comparison and only the mean is present. The visual cloud presented in Figure 15(b) illustrates that drug addicts in their after shot have a noticeable positive increment in the asymmetry metrics where they are almost separable from the rest of the samples.

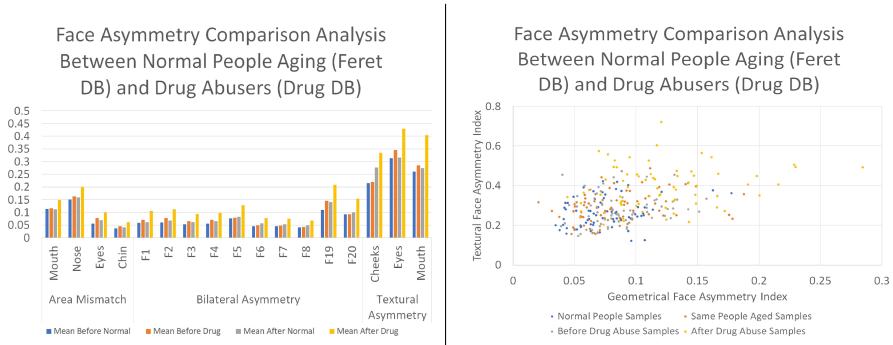

(a) comparison statistics

(b) comparison cloud

Figure 15: Demonstrative charts comparing the statistical results on facial asymmetry analysis on the Drug Addicts and the FERET databases: (a) bar graph representing statistical results from geometrical and textural analysis, (b) a cloud representation of the samples for geometrical vs textural face asymmetry

Metric/Database	FERET (normal people aging)			Drug-addicts (drug addicts aging)		
	Before	After	Asymmetry Increment	Before	After	Asymmetry Increment
Geometrical asymmetry mean	7%	8%	1%	8%	13%	**5%**
Textural asymmetry mean	26%	29%	3%	28	39	**11%**

Table 4: Average face asymmetry of the employed assessment metrics on the FERET and Meth-Addicts databases

4. Discussions

We collected a database of meth addicts for investigating long-term effects of meth abuse and addiction on face asymmetry, compared with a control database of ordinary people aging.

Generally, the task of assessing facial asymmetry consists of two parts: determining a symmetry plane which fits best to the present partial bilateral symmetry and quantifying the amount of violation of this symmetry. Several machine-learning-based methods perform the first part with high-accuracy, e.g., the Dlib face landmarks extractor [21] used in this work. In contrast, the second part of the task is not straight forward; actually, existent methods for quantify-

ing face asymmetry were found to have a low scoring correlation in [11]. Hence, in our comparison of facial asymmetry, we combine the two most credible methods in the literature for assessing geometrical asymmetry, namely, the bilateral features and the area mismatch. Additionally, for supporting the hypothesis, we employ a new metric for assessing textural face asymmetry using the structural similarity index (SSIM).

All three metrics mentioned above showed consistency in their indications; with the major indication being a significant increment of facial asymmetry for meth addicts while aging, three to five times more than ordinary people (Table 4). These findings align with a medical evidence on how meth abuse and addiction cause several face distortions [2, 3] as summarized in Section 1.1.

At this point, we would like to bring to the reader's attention that most of the facial images analyzed for meth-addicts were collected by the US police authority in the faces of meth project [15]. Undoubtedly, this database is one of a kind, acknowledging that it gathers a significant population of meth-addicts at two different stages of meth abuse for each of its members. Consequently, this database was welcomed by the research community and employed in different face analysis researches on drug abuse as in [4, 5, 6, 7]. However, it remains possible that the police authority selected particular cases to achieve a deterrent effect on meth abuse. Therefore, the increase in facial asymmetry among meth addicts could be lower on average than what we estimated in this research.

Conclusively, each of the faces we analyzed in this work shows some degree of asymmetry. This finding is consistent with the results in [19]; where they used an optical-flow approach based on four bilateral features and analyzed 4000 face images.

On the one hand, the results we obtained on the aging of ordinary people using bilateral features on the FERET database are semi-identical to the ones obtained in [8]; more specifically, we both concluded that face asymmetry increases in aging by employing this metric. The difference between their work and ours is the new step we performed of calculating the percentage of asymmetry increase. Also, both results showed that the geometrical asymmetry in

the lower part of the face is more affected in aging. On the other hand, in this work, we extended these findings to show that textural-wise asymmetry around the cheeks area increases the most with aging.

Moreover, in relation to the existing literature, both the purpose of the study and employed tools align with previous works on face symmetry distortion. In [10], they show an increment of facial asymmetry for rhabdomyosarcoma survivors caused by medical therapy by combining bilateral features with surveys (human-opinion based). Where in [16] and [17], they analyzed face asymmetry for cleft lip and palate patients and defined an aesthetic range for lip and nose features respectively, both works used the area mismatch-based metric of nose and lip areas using software known by Symnose. Similarly, in this work, we combine bilateral features and an area-mismatch based metric to give a score on geometrical face asymmetry. It is worth mentioning that regarding the area mismatch metric, the existing software (Symnose) requires a manual annotation for the region where symmetry analysis is concerned, wherein this work, we automated the usage of this metric using face feature extraction.

However, automating an area mismatch-based and a textural-based face asymmetry assessment metrics are original contributions of this research. Although they were tailored to serve for this research, their concepts can be generally adapted for face asymmetry assessment. Interestingly enough, few researchers built specific-to-their-need tools to analyze facial asymmetry. Although in most of the cases such tools are not applicable on a general scope, however, they opened the door for new methods to be accepted for this purpose. Notably, in [14], a method based on Optimal Symmetry Planes (OSP) of CT scans was introduced for studying the correlation between face asymmetry and jawbone asymmetries. Also, in [18], a wavelet-based method for 2D images was introduced to give a signature of faces based on an acceptable range of face symmetry.

Noteworthy, two limitations are associated with this study. Firstly, A new database named as PCSO_LS has been recently collected and employed in [7] for aging studies, and is considered as the most populated aging database so

far [1]. This database could serve in this research as a control database besides the FERET database that we employed. However, PCSO_LS was not made public up to today, and our attempts for obtaining this database were fruitless. Secondly, the number of detected landmarks of all available face-landmarks extractor is somehow limited, e.g., the Dlib landmark detector used in this work detects twenty landmarks on the mouth, nine on the nose and six on the eyes. Which in turn results in "bulky" contouring when the area mismatch metric is concerned (see Figure 6). However, if PSSO_LS becomes publicly available, or when the technology of face landmarks-detecting evolves, it would be an interesting task to employ in improving the quality of our area mismatch metric and our findings.

Finally, this study is one of a kind undertaken to date in the context of analyzing long term effects of meth abuse on face asymmetry. Therefore, its findings may serve as a benchmark for different face-analysis-related future researches in general, and face recognition for drug addicts in specific. In fact, face recognition was found to be highly dependent on facial symmetry in [20], and, face recognition systems were found to perform poorly on drug addicts in [4, 5, 6], hence, one might persuade the findings of this work in building better performing recognition systems on drug addicts.

4.1. On the face asymmetry assessment from 3D imaging

Three-dimensional (3D) imaging technologies have broadly evolved in the last decade. Remarkably, several themes of research started to take place on quantifying facial asymmetry using advanced medical imaging tools (e.g., computerized tomography (CT) scans [23]). However, the surface of the face remains the most powerful channel for human interaction and the most significant area that clinicians consider as the basis of aesthetic perception. Hence, facial asymmetry assessment using 3D surface imaging is the new mainline dominating recent research in the medical field and dentistry [24].

In the following, we discuss possible extensions of the method we employed for geometrical facial asymmetry assessment on 2D images to 3D surface images.

Still, since we lack suitable databases for faces on drug abuse or aging, the purpose of this paragraph is to provide the reader with solid concepts on the potential solutions for facial asymmetry assessment using 3D surfaced meshes, which can help future researchers analyzing future databases. In the following, we provide explanations on an illustrative toy example, by reconstructing a 3D view from an available 2D face image for explaining how 3D facial asymmetry analysis can be performed in the same context.

Several methods exist for retrieving 3D information of the face from a single image [25]. Shape-from-shading [26], 3D Morphable Model (3DMM) [27], structure from motion [28] and learning-based methods [29] are some of the most important ones. Having considered that only frontal view images are available in our databases, we reconstruct a 3D face using a single 2D frontal image using the method proposes in [30]. This method provides an automatic estimation of the 3D shape and texture of a given face. Briefly, each frontal 2D image of an individual is projected onto a vector space representation of 3D faces. An error rate arises due to the estimation of Z coordinate since we did not have access to profile views of faces. We compensate for this error by considering $\pm \Delta$ as a correction parameter (this parameter can be rectified in case of better 3D reconstruction from multiple views).

Performing 3D facial asymmetry analysis requires characteristic landmark points. Several similar-in-concept approaches were introduced for landmarks localization on 3D faces for use in face recognition applications. Colombo et al. [31] identified the eyes and nose of the individuals to perform 3D face detection. Gordon [32] performed a precise face analysis for face alignment based on curvatures of extracted features on nose tip, nose bridge, and eyes corners. An algorithm was developed by Colbry et al. [33] to detect face anchor points using 3D models for verification to estimate the pose and then match a test face to a 3D face model. Using the same concepts in the existing literature, we extract characteristic landmarks to perform facial asymmetry assessment by discovering maximum and minimum local curvatures. Specifically, we extracted the points on the eyes (middle canthus), the tip of the nose, around the lip (namely: oral

commissures, cupid's bow, and lower vermillion border), as well as the chin, and middle of the eyes (nasion) by discovering the maximum and minimum local curvatures. Consequently, we obtained eleven craniofacial landmark coordinates on 3D face mesh. These eleven landmarks partially correspond to those extracted in 2D in Section 2.2.1.

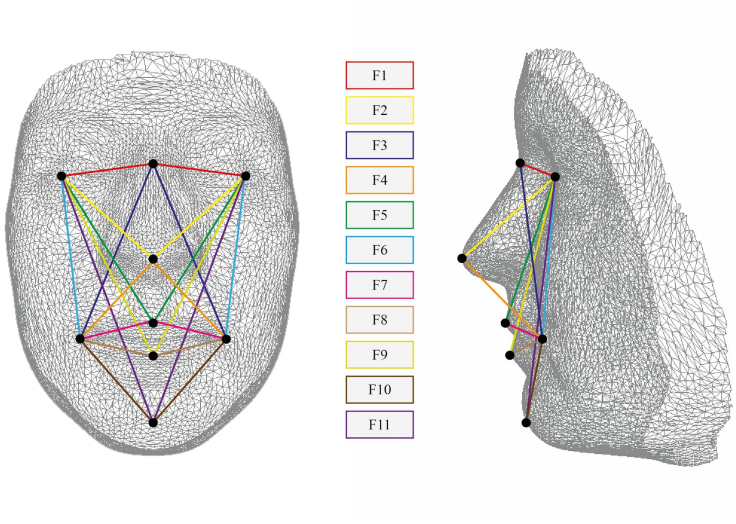

Figure 16: Employed bilateral features on 3D face mesh for face asymmetry analysis

Using the same concept of the bilateral asymmetry approach in 2D, we construct a 3D bilateral asymmetry features on a face mesh based on selected Euclidean distances between these landmarks. A visual illustration on the employed landmarks and the resultant features is present in Figure 16, where eleven bilateral features referred to as $F1, F2, ..., F11$ are considered on the 3D face mesh. Each feature corresponds to a distance difference, between a landmark in the middle of the face, and its left and right feature points. For instance, $F1$ indicates the difference distance from the nasion point, to the left mid-canthus and right mid-canthus. We represent these features in percentages to facilitate future statistical analysis for asymmetry measurements.

An example of the bilateral asymmetry metric applied on two 3D faces of the same person in the early, and late stages of drug abuse (before and after) is

demonstrated in Figure 17. We can visualize the changes in facial appearance in both texture and shape, and the results of asymmetry measurements applying the bilateral feature assessment are given in the table. Coherently with the results obtained from 2D assessment, we notice that for each 3D bilateral feature, there has been a slight increase in the obtained values, which brings about proof of concept of our example 3D bilateral features on future 3D face databases.

Feature	Before (%) ± Δ
F1	3.64
F2	3.94
F3	3.35
F4	1.66
F5	2.34
F6	1.81
F7	4.83
F8	7.06
F9	1.47
F10	2.72
F11	1.12

Feature	After (%) ± Δ
F1	**4.75**
F2	**4.14**
F3	**3.78**
F4	**2.85**
F5	**2.52**
F6	**2.32**
F7	**6.12**
F8	**8.51**
F9	**1.81**
F10	**3.57**
F11	**1.20**

Figure 17: Example of bilateral asymmetry features applied on a person in the early and late stages of drug abuse

5. Summary and conclusions

We presented a 2D (two dimensional) geometrical and textural based face asymmetry analysis for the comparison of normal vs drug life aging. The employed tools combined both local and global analysis for face geometry, inspired from the most credible state-of-the-art in the field, namely: bilateral features for local geometrical analysis, area mismatch for global geometrical analysis and structural similarity index for carefully cropped dual face regions for textural asymmetry. We also provided a detailed discussion on the extension to 3D for an assessment of 3D facial asymmetry has been demonstrated to show the potential solutions of objective asymmetry assessments employing 3D surfaced meshes of the human face. The statistical analysis shows the following points:

- For ordinary people, the asymmetry in faces slightly increases by aging. Where, our asymmetry measure points to a 1% increase in geometrical asymmetry and a 3% increase in textural asymmetry, with a maximum increase in the cheeks area.
- For drug addicts, the asymmetry in faces is relatively exaggerated. Where our asymmetry measure points to a 5% increase in geometrical asymmetry and an 11% increase in textural asymmetry.

The data on hand and the employed tools gives an affirmative answer to the question "does meth abuse and addiction affect face symmetry?".

6. Conflicts of interest

The authors declare that they have no conflicts of interest.

References

[1] M. M. Sawant, K. M. Bhurchandi, Age invariant face recognition: a survey on facial aging databases, techniques and effect of aging, Artificial Intelligence Review (2018) 1–28.

[2] T. E. Freese, K. Miotto, C. J. Reback, The effects and consequences of selected club drugs, Journal of substance abuse treatment 23 (2) (2002) 151–156.

[3] NIDA, Methamphetamine, (Accessed February 19, 2019).
URL `www.drugabuse.gov/publications/drugfacts/methamphetamine`

[4] D. Yadav, N. Kohli, P. Pandey, R. Singh, M. Vatsa, A. Noore, Effect of illicit drug abuse on face recognition, in: 2016 IEEE Winter Conference on Applications of Computer Vision (WACV), IEEE, 2016, pp. 1–7.

[5] R. Raghavendra, K. B. Raja, C. Busch, Impact of drug abuse on face recognition systems: a preliminary study, in: Proceedings of the 9th International Conference on Security of Information and Networks, ACM, 2016, pp. 24–27.

[6] R. Ramachandra, K. Raja, S. Venkatesh, C. Busch, Collaborative representation of statistically independent filters' response: An application to face recognition under illicit drug abuse alterations, in: Scandinavian Conference on Image Analysis, Springer, 2017, pp. 448–458.

[7] L. Best-Rowden, A. K. Jain, Longitudinal study of automatic face recognition, IEEE transactions on pattern analysis and machine intelligence 40 (1) (2018) 148–162.

[8] M. Sajid, I. A. Taj, U. I. Bajwa, N. I. Ratyal, The role of facial asymmetry in recognizing age-separated face images, Computers & Electrical Engineering 54 (2016) 255–270.

[9] K. Bachi, S. Sierra, N. D. Volkow, R. Z. Goldstein, N. Alia-Klein, Is biological aging accelerated in drug addiction?, Current opinion in behavioral sciences 13 (2017) 34–39.

[10] R. A. Schoot, M. L. Hol, J. H. Merks, M. Suttie, O. Slater, M. van Lennep, S. M. Hopman, D. Dunaway, J. Syme-Grant, L. E. Smeele, et al., Facial asymmetry in head and neck rhabdomyosarcoma survivors, Pediatric blood & cancer 64 (10) (2017) e26508.

[11] D. G. Mosmuller, T. J. Maal, C. Prahl, R. A. Tan, F. J. Mulder, R. M. Schwirtz, H. C. de Vet, S. J. Bergé, J. D. Griot, Comparison of two-and three-dimensional assessment methods of nasolabial appearance in cleft lip and palate patients: Do the assessment methods measure the same outcome?, Journal of Cranio-Maxillofacial Surgery 45 (8) (2017) 1220–1226.

[12] G. Thiesen, B. F. Gribel, M. P. M. Freitas, Facial asymmetry: a current review, Dental press journal of orthodontics 20 (6) (2015) 110–125.

[13] T. T. Wang, L. Wessels, G. Hussain, S. Merten, Discriminative thresholds in facial asymmetry: a review of the literature, Aesthetic surgery journal 37 (4) (2017) 375–385.

[14] T.-Y. Wong, J.-K. Liu, T.-C. Wu, Y.-H. Tu, K.-C. Chen, J.-J. Fang, K.-H. Cheng, J.-W. Lee, Plane-to-plane analysis of mandibular misalignment in patients with facial asymmetry, American Journal of Orthodontics and Dentofacial Orthopedics 153 (1) (2018) 70–80.

[15] M. C. S. Office, Faces of meth, (Accessed February 19, 2019).
URL www.mcso.us/facesofmeth

[16] N. S. Kornmann, R. A. Tan, F. J. Mulder, J. T. Hardwicke, B. M. Richard, B. B. Pigott, R. W. Pigott, Defining the aesthetic range of normal symmetry for lip and nose features in 5-year-old children using the computer-based program symnose, The Cleft Palate-Craniofacial Journal (2018) 1055665618813236.

[17] R. W. Pigott, B. B. Pigott, Quantitative measurement of symmetry from photographs following surgery for unilateral cleft lip and palate, The Cleft Palate-Craniofacial Journal 47 (4) (2010) 363–367.

[18] G. Passalis, P. Perakis, T. Theoharis, I. A. Kakadiaris, Using facial symmetry to handle pose variations in real-world 3d face recognition, IEEE Transactions on Pattern Analysis and Machine Intelligence 33 (10) (2011) 1938–1951.

[19] J. Chen, C. Yang, Y. Deng, G. Zhang, G. Su, Exploring facial asymmetry using optical flow, IEEE Signal Processing Letters 21 (7) (2014) 792–795.

[20] J. Chen, C. Xia, H. Ying, C. Yang, G. Su, Using facial symmetry in the illumination cone based 3d face reconstruction, in: 2013 IEEE International Conference on Image Processing, IEEE, 2013, pp. 3700–3704.

[21] V. Kazemi, J. Sullivan, One millisecond face alignment with an ensemble of regression trees, in: Proceedings of the IEEE conference on computer vision and pattern recognition, 2014, pp. 1867–1874.

[22] C. Sagonas, E. Antonakos, G. Tzimiropoulos, S. Zafeiriou, M. Pantic, 300 faces in-the-wild challenge: Database and results, Image and vision computing 47 (2016) 3–18.

[23] T.-Y. Wong, J.-K. Liu, T.-C. Wu, Y.-H. Tu, K.-C. Chen, J.-J. Fang, K.-H. Cheng, J.-W. Lee, Plane-to-plane analysis of mandibular misalignment in patients with facial asymmetry, American Journal of Orthodontics and Dentofacial Orthopedics 153 (1) (2018) 70–80.

[24] A. Patel, S. M. S. Islam, K. Murray, M. S. Goonewardene, Facial asymmetry assessment in adults using three-dimensional surface imaging, Progress in orthodontics 16 (1) (2015) 36.

[25] M. Aboali, N. A. Manap, A. M. Darsono, Z. M. Yusof, Review on three-dimensional (3-d) acquisition and range imaging techniques, Int. J. Appl. Eng. Res 12 (2017) 2409–2421.

[26] M. Castelan, E. R. Hancock, Acquiring height maps of faces from a single image, in: Proceedings. 2nd International Symposium on 3D Data Processing, Visualization and Transmission, 2004. 3DPVT 2004., IEEE, 2004, pp. 183–190.

[27] V. Blanz, T. Vetter, et al., A morphable model for the synthesis of 3d faces., in: Siggraph, Vol. 99, 1999, pp. 187–194.

[28] J. Fortuna, A. M. Martinez, Rigid structure from motion from a blind source separation perspective, International journal of computer vision 88 (3) (2010) 404–424.

[29] M. Song, D. Tao, X. Huang, C. Chen, J. Bu, Three-dimensional face reconstruction from a single image by a coupled rbf network, IEEE Transactions on Image Processing 21 (5) (2012) 2887–2897.

[30] V. Blanz, T. Vetter, Face recognition based on fitting a 3d morphable model, IEEE Transactions on pattern analysis and machine intelligence 25 (9) (2003) 1063–1074.

[31] A. Colombo, C. Cusano, R. Schettini, 3d face detection using curvature analysis, Pattern recognition 39 (3) (2006) 444–455.

[32] G. G. Gordon, Face recognition based on depth maps and surface curvature, in: Geometric Methods in Computer Vision, Vol. 1570, International Society for Optics and Photonics, 1991, pp. 234–247.

[33] D. Colbry, G. Stockman, A. Jain, Detection of anchor points for 3d face veri. cation, in: 2005 IEEE Computer Society Conference on Computer Vision and Pattern Recognition (CVPR'05)-Workshops, IEEE, 2005, pp. 118–118.